Global Change Biology (2007) **13,** 652–670, doi: 10.1111/j.1365-2486.2006.01225.x

Estimating parameters in a land-surface model by applying nonlinear inversion to eddy covariance flux measurements from eight FLUXNET sites

YING PING WANG*, DENNIS BALDOCCHI†, RAY LEUNING‡, EVA FALGE§ and TIMO VESALA¶

*CSIRO Marine and Atmospheric Research, Private Bag #1, Aspendale, Vic. 3195, Australia, †Department of Environmental Sciences, Policy and Management, Ecosystem Science Division, 151 Hilgard Hall, University of California, Berkeley, CA 94720-3110, USA, ‡CSIRO Marine and Atmospheric Research, FC Pye Lab, GPO Box 1666, Canberra, ACT 2601, Australia, §Plant Ecology, University of Bayreuth, 95440 Bayreuth, Germany, ¶Department of Physical Sciences, University of Helsinki, FIN-00014, PO Box 64, Finland

Abstract

Flux measurements from eight global FLUXNET sites were used to estimate parameters in a process-based, land-surface model (CSIRO Biosphere Model (CBM), using nonlinear parameter estimation techniques. The parameters examined were the maximum photosynthetic carboxylation rate ($v_{cmax,25}$) the potential photosynthetic electron transport rate ($j_{max,25}$) of the leaf at the top of the canopy, and basal soil respiration ($r_{s,25}$), all at a reference temperature of 25 °C. Eddy covariance measurements used in the analysis were from four evergreen forests, three deciduous forests and an oak-grass savanna. Optimal estimates of model parameters were obtained by minimizing the weighted differences between the observed and predicted flux densities of latent heat, sensible heat and net ecosystem CO_2 exchange for each year. Values of maximum carboxylation rates obtained from the flux measurements were in good agreement with independent estimates from leaf gas exchange measurements at all evergreen forest sites. A seasonally varying $v_{cmax,25}$ and $j_{max,25}$ in CBM yielded better predictions of net ecosystem CO_2 exchange than a constant $v_{cmax,25}$ and $j_{max,25}$ for all three deciduous forests and one savanna site. Differences in the seasonal variation of $v_{cmax,25}$ and $j_{max,25}$ among the three deciduous forests are related to leaf phenology. At the tree-grass savanna site, seasonal variation of $v_{cmax,25}$ and $j_{max,25}$ was affected by interactions between soil water and temperature, resulting in $v_{cmax,25}$ and $j_{max,25}$ reaching maximal values before the onset of summer drought at canopy scale. Optimizing the photosynthetic parameters in the model allowed CBM to predict quite well the fluxes of water vapor and CO_2 but sensible heat fluxes were systematically underestimated by up to 75 W m^{-2}.

Keywords: CBM, FLUXNET, inversion, latent, parameter, photosynthesis, sensible heat flux

Received 20 December 2005; revised version received 12 May 2006 and accepted 12 May 2006

Introduction

For several decades now, measurements at leaf, plant and canopy scale have been used to develop, test and parameterize process-based land-surface models used to study climate–biosphere interactions (Dickinson, 1983; Sellers *et al*., 1996). In those models, global vegetation is typically classified into different biome types, and look-up tables are used to provide estimates of model parameters for each biome (e.g. Sellers *et al*., 1996). The parameters have generally been derived from small numbers of measurements at the plant or field scale or from expert judgment. However, problems can arise when parameters derived at one scale are used to estimate fluxes at a larger scale due to nonlinear relationships between model parameters and the fluxes and stores in land-surface scheme. In this case, parameters obtained at the leaf or plant scale will not be applicable at larger scales and it is then necessary to simplify and linearize the models, develop aggregation

Correspondence: Yingping Wang, tel. + 61 3 9239 4577, e-mail: yingping.wang@csiro.au

rules from one scale to another, or to estimate parameters at the scale at which projections are required. Because of the complexities which arise in scaling from leaf to a canopy (Field *et al*., 1995; Leuning *et al*., 1995; Wang & Leuning, 1998), it may be better to estimate model parameters using ecosystem-scale measurements for regional or global applications, rather than using leaf-level parameters. Some parameters may vary seasonally (Wilson *et al*., 2001; Xu & Baldocchi, 2003), so intermittent field measurements such as leaf gas exchange, may not correctly capture their seasonal variations. In contrast, continuous eddy covariance flux measurements provide a unique opportunity to examine the magnitude and dynamics of seasonal change in some key parameters in land-surface models, and the global FLUXNET database allows examination of parameter variation across diverse biomes and climates.

Sellers *et al*. (1996) identified nine key physiological parameters as being strongly biome dependent in their land-surface model. They found that maximum photosynthetic carboxylation rate and minimum stomatal conductance were the most variable among biomes, which suggests that these parameters need to be well defined for a range of biomes globally. Photosynthetic capacity is also a key parameter in the two leaf, CSIRO Biosphere Model (CBM) through the close coupling of photosynthesis and stomatal conductance, which affects energy partitioning, transpiration and CO_2 exchange (Leuning *et al*., 1995). Wang *et al*. (2001) found that bulk estimates of the photosynthetic carboxylation rate and the electron transport rate at the reference temperature of 25 °C ($v_{c_{\max},25}$, and $j_{\max,25}$, respectively), can be used to calculate accurately canopy photosynthesis and energy fluxes. They also showed that these fluxes can be accurately predicted by the two-leaf model for a mixture of two different vegetation types if the $v_{c_{\max}}$ and $j_{\max}$ values for each type are weighted using their respective canopy leaf area index (LAI).

Process-based models usually require a large number of parameters, only some of which can be estimated from eddy flux data. The exact number of parameters that can be extracted using nonlinear optimization depends on the model used in the optimization and quality of the measurements. If too many parameters are estimated, the optimization will either not converge or it will converge to a local minimum because of strong correlations between different parameters. If too few parameters are chosen, some information in the measurements will not be extracted by the optimization, and the estimates of the optimized parameters may be sensitive to the values of the fixed parameters. This problem can be partially resolved by constraining some of the parameters using relatively small prior uncertainties rather than fixing them, or selecting parameters that are well constrained by measurements. Wang *et al*. (2001) examined the constraints provided by eddy flux data on parameters in CBM and concluded that only three to five parameters can be estimated independently using eddy flux measurements of sensible heat, water vapor and CO_2 because of the close coupling of canopy photosynthesis and latent heat fluxes. On the other hand, measurements of energy fluxes helped to distinguish between limitations of canopy photosynthesis caused by stomatal conductance (the supply function) and photosynthetic capacity (demand function), because canopy latent heat flux can be limited by stomatal conductance but only indirectly by photosynthetic capacity.

Braswell *et al*. (2005) applied nonlinear inversion to the eddy covariance flux measurements from Harvard forest using a simplified model of photosynthesis and evapotranspiration, and concluded that the multiple-year eddy covariance flux measurements provide tight constraints on photosynthetic parameters, but rather poor constraints on parameters relating to soil decomposition that varies at considerably longer time scale than canopy photosynthesis and transpiration. Willaims *et al*. (2005) also concluded that long-term measurements of carbon pool sizes are required to estimate the parameters relating to decomposition of soil organic matter. Aalto *et al*. (2004) estimated two-key parameters in their global biosphere model by applying nonlinear inversion to eddy flux measurements and satellite measurements of NDVI for 13 FLUXNET sites in Europe, even though the actual number of parameters needed by the model for each biome is far greater than two.

Over 250 flux towers are now installed worldwide to monitor the fluxes of radiation, heat, water vapor and CO_2 (FLUXNET, Baldocchi *et al*., 2001). The global network of long-term eddy flux stations continues the pioneering work of Wofsy *et al*. (1993) who established the first continuous measurements of surface fluxes in the Harvard forest. Data collected from flux towers have been used to study the diurnal and seasonal variations of surface fluxes and energy partitioning within different forest types (e.g. Black *et al*., 1996; Goulden *et al*., 1996; Valentini *et al*., 1996; Falge *et al*., 2001; Wilson *et al*., 2002, 2003; Leuning *et al*., 2005). We have learnt a great deal about how plant functional types respond to weather and soil conditions at canopy scale (e.g. Baldocchi *et al*., 2004), and which factors control seasonal and interannual variations of exchanges of carbon, water and heat between land surface and lower atmosphere (Valentini *et al*., 2000; Baldocchi *et al*., 2001). This study builds on previous experience and understanding of using eddy flux data to develop a framework for nonlinear parameter estimation and to use the framework to estimate key model parameters in

CBM using data from eight FLUXNET sites. The results are used to examine seasonal variation in the parameters and to identify systematic errors in the model.

Methodology

Optimization

The relationship between the parameters ($\boldsymbol{P}$) in CBM and the predicted surface fluxes ($\boldsymbol{Y}$) is

$$\boldsymbol{Y} = f(\boldsymbol{P}, \boldsymbol{M}), \quad (1)$$

where $\boldsymbol{M}$ represents the meteorological forcing, and f represents CBM. The parameters were estimated by minimizing the cost function (ϕ) that was constructed as

$$\phi = \frac{1}{2}(\boldsymbol{Y}-\boldsymbol{O})^{\mathrm{T}}\boldsymbol{C}_0^{-1}(\boldsymbol{Y}-\boldsymbol{O}) + \frac{1}{2}((x-x_{\mathrm{prior}}/C)_x)^2, \quad (2)$$

where $\boldsymbol{O}$ is the vector of observed surface fluxes, x is the estimate of the ratio $j_{\mathrm{max},25}/v_{\mathrm{c_{max},25}}$ during the optimization, x_{prior} is the prior estimate of x, $\boldsymbol{C}_0$ is the covariance of observed surface fluxes and C_x is the variance of the prior estimate of x. In this study, we used the Marquardt–Levenberg method as implemented in the nonlinear parameter estimation program PEST (Doherty, 2002) to find the minimum value of ϕ. The covariance of the estimates of parameter $\boldsymbol{P}$, denoted $\boldsymbol{C}_{\mathrm{p}}$, is calculated as

$$\boldsymbol{C}_{\mathrm{p}}^{-1} = \boldsymbol{J}_0\boldsymbol{C}_0^{-1}\boldsymbol{J}_0^{\mathrm{T}} + \boldsymbol{J}_x C_x^{-1}\boldsymbol{J}_x^{\mathrm{T}}, \quad (3)$$

where $\boldsymbol{J}_0$ is the first derivative of an observation ($\boldsymbol{O}$) with respect to $\boldsymbol{P}$, and $\boldsymbol{J}_x$ is the first derivative of x with respect to parameters $\boldsymbol{P}$.

Sensitivities of observations to model parameters ($\boldsymbol{J}_0$) and x to $\boldsymbol{P}$ ($\boldsymbol{J}_x$) are calculated using the central difference method (Doherty, 2002), and both are model dependent. The quality of the measurements and prior knowledge of x is quantified by the observation covariance ($\boldsymbol{C}_0$) and uncertainty of x_{prior} (C_x). Equation (3) shows that the uncertainty of the parameter estimates increases with $\boldsymbol{C}_0$ and C_x, and decreases with the first derivatives ($\boldsymbol{J}_0$ and $\boldsymbol{J}_x$). Therefore, only those parameters that are sufficiently sensitive to observations can be reliably determined by the optimization.

The second term on the right-hand side of Eqn (2) represents the prior information used in the optimization. Wullschleger (1993) found a strong correlation between two photosynthetic parameters, the maximum carboxylation rate ($v_{\mathrm{cmax},25}$) and maximum potential electron transport rate ($j_{\mathrm{max},25}$). Analysis by Leuning (2002) suggested that the ratio $x(=j_{\mathrm{max},25}/v_{\mathrm{max},25})$ at leaf scale is about 2.7, a finding that is supported by physiological arguments (Medlyn, 1996). We studied the sensitivity of the unexplained residuals (the first term on the right-hand side of Eqn (2)) to values of C_x varying from 0.01 to 10.0. As the weighting factor, $1/C_x$, increases, the contribution of prior information to x decreases, and estimates of x can differ significantly from $x_{\mathrm{prior}} = 2.7$, which is inconsistent with many field and laboratory studies. We found that $C_x = 0.1$ gives estimates of x between 2 and 4 for the eight sites studied.

Table 1 Initial values and ranges of model parameters optimized in this study

Parameter	Unit	Initial value	Range
α_{L}	–	1.0	0.8–1.0
$\alpha_{j\mathrm{max},25}$	–	1.0	0.1–5.0
$j_{\mathrm{max},25}/v_{\mathrm{cmax},25}$	–	2.0	1.8–2.2
$\alpha_{\mathrm{rs},25}$	–	1.0	0.01–50
T_{o}	°C	20	0–50
ΔT	°C	20	0–100

To maximize computational efficiency when using PEST, a site-independent optimization strategy was developed that could use eddy flux measurements from any selected site. The required site-specific information is included in the parameter input file needed to run the land-surface model. This is important if we want to compare estimates of parameters from different sites and obtain parameter estimates that can be used in global modeling. Site independence was achieved by normalizing each parameter to be optimized by its initial value, that is $\boldsymbol{\alpha} = \boldsymbol{P}/\boldsymbol{P}_0$, where $\boldsymbol{P}_0$ represents the initial value of parameter and may be site specific. The ratio $\boldsymbol{\alpha}$ is thus optimized, rather than the parameters $\boldsymbol{P}$ themselves. The same initial values and prior uncertainties of α were used in the optimizations for all sites, and are listed in Table 1. Final estimates of $\boldsymbol{P}$ are calculated as $\boldsymbol{\alpha}^{\mathrm{T}}\boldsymbol{P}_0$. No significant differences in the parameter estimates and their uncertainties were found when the optimization was repeated with several different initial values.

Seasonal variation in several parameters was determined using data time series of varying length. To test whether the cost, ϕ, is significantly different for CBM with (subscript k) or without (subscript l) the seasonal variations of $v_{\mathrm{cmax},25}$, the χ^2 value were calculated as

$$\chi^2 = \frac{\phi_{\mathrm{k}} - \phi_{\mathrm{l}}}{\phi_{\mathrm{l}}}\frac{df_{\mathrm{l}}}{df_{\mathrm{k}} - df_{\mathrm{l}}}, \quad (4)$$

where df is the number of degrees of freedom, calculated as $\sum_{j=1,2,3} n_j - m$, where n_j is total number of flux measurements, for latent heat ($j = 1$), sensible heat ($j = 2$) and CO_2 ($j = 3$), and m is the number of optimized parameters.

An agreement index, d, developed by Willmott (1984) is used to describe the agreement between model prediction using the optimal estimates of parameters and observations. Values of 0 or 1 represent no or perfect agreement, respectively.

CBM and its parameterization for each FLUXNET site

CBM simulates the fluxes of latent and sensible heat and net ecosystem CO_2 exchange. It consists of submodels of (1) canopy radiation transfer using a simplified two-stream approximation (Spitters, 1986; Wang & Leuning, 1998; Wang, 2003), (2) atmospheric transport using the simplified localized near-field turbulence theory of Raupach *et al*. (1997), (3) a two-leaf (sunshade) model that fully couples photosynthesis, stomatal conductance, transpiration, and leaf energy balances (Leuning *et al*., 1995; Wang & Leuning, 1998) and (4) a module that simulates water and heat transfer within soil and snow (Kowalczyk *et al*., 1994). CBM is the land-surface scheme in the CSIRO global climate model, and an international comparisons of various such schemes found that CBM provided excellent simulations of the fluxes of heat, water vapor and CO_2 (Pitman *et al*., 1999).

The measured net exchanges of latent heat, F_e, and sensible heat, F_h, are given by the sum of fluxes from the canopy (subscript c) and the soil (subscript s)

$$F_e = F_{ec} + F_{es}, \tag{5}$$

$$F_h = F_{hc} + F_{hs}. \tag{6}$$

Net ecosystem CO_2 exchange, F_c, is calculated as the sum of three component fluxes: canopy net photosynthesis, A_n, nonleaf respiration, R_p, and soil respiration, R_s:

$$F_c = A_n + R_p + R_s, \tag{7}$$

where F_c is negative for CO_2 uptake by the terrestrial biosphere. The two-leaf canopy model described by Wang & Leuning (1998) fully couples photosynthesis, stomatal conductance, transpiration and leaf energy balances (Leuning *et al*., 1995). This recognizes that stomata provide the primary passage for the transport of water vapor and CO_2 between the leaf and ambient air (Cowan & Farquhar, 1977), thereby controlling the partitioning of energy between F_{ec} and F_{hc}. Key parameters in the photosynthesis model include the maximum carboxylation rate of the enzyme Rubisco, $v_{cmax,25}$, and maximum potential electron transport rate, $j_{max,25}$, at a leaf temperature of 25 °C. The stomatal model has two empirical parameters, a and D_0, which describe the sensitivity of stomatal conductance to the net photosynthesis rate and the humidity deficit of the atmosphere. Following Leuning *et al*. (1995), the relationship between A_n and stomatal conductance, G_c, is given by

$$G_c = G_{c0} + \frac{aA_n}{(C_s - \Gamma)(1 + D_s/D_0)}, \tag{8}$$

where C_s is CO_2 concentration at the leaf surface ($\mu mol\,mol^{-1}$), Γ is the CO_2 compensation point of photosynthesis ($\mu mol\,mol^{-1}$), D_s is water vapor pressure deficit at the leaf surface (Pa), and G_{c0} is conductance of the leaves ($\mu mol\,m^{-2}\,s^{-1}$) when $A_n = 0$. Equation (8) is applied to sunlit and shaded leaves separately.

Respiration from woody tissue and roots (R_p) is modeled as

$$R_p = 0.7 r_{p,25} Q_{10}^{(T_p - 20)/10}, \tag{9}$$

where $r_{p,25}$ is the basal respiration rate at 25 °C, coefficient 0.7 represents the ratio of R_p at 20 and 25 °C, and Q_{10} decreases with an increase in plant tissue temperature in °C (T_p) according to Tjoelker *et al*. (2001):

$$Q_{10} = 3.22 - 0.046 T_p. \tag{10}$$

As R_p does not include leaf respiration that is included in calculating A_n, respiration from roots will contribute to most of R_p. Studies have shown that Q_{10} formulation is quite adequate for modeling the response of R_p to temperature (Reichstein *et al*., 2005). To calculate R_p it is assumed that T_p, is equal to ambient air temperature (T_a) in this study.

Soil respiration or heterotrophic respiration, R_s, is modeled as a function of soil temperature and moisture using

$$R_s = r_{s,25} f_1(\overline{T_s}) f_2(\overline{v_s}), \tag{11}$$

where $r_{s,25}$ is the soil respiration rate at soil temperature ($\bar{T}_s$) of 25 °C with no water stress ($f_2 = 1$), and where functions f_1 and f_2 describe the dependence of soil respiration on T_s, the mean soil temperature (°C) and on v_s, the mean fraction of water-filled pore space, weighted by root mass fraction in all six soil layers. The functions used are

$$f_1(\overline{T_s}) = 2.43 \exp\left(\frac{3.36(\overline{T_s} - 40)}{\overline{T_s} + 31.79}\right), \tag{12}$$

$$f_2(\bar{v}_s) = 3.63\bar{v}_s - 3.20\bar{v}_s^2 - 0.12\bar{v}_s^3. \tag{13}$$

Equations (12) and (13) are taken from Kirschbaum (1995) and from Kelly *et al*. (2000), respectively.

Submodels for seasonal variation of maximum carboxylation rate

Maximum carboxylation rate (v_{cmax}) and maximum potential electron transport rate (j_{max}) of the leaves at the top of the canopy are calculated as

$$v_{cmax} = v_{cmax,25} f_{T,v} f_d f_w = v_{x,25} f_{T,v}, \quad (14)$$

$$j_{max} = j_{max,25} f_{T,j} f_d f_w = j_{x,25} f_{T,j}, \quad (15)$$

where $v_{cmax,25}$ and $j_{max,25}$ are the corresponding values at a leaf temperature of 25 °C. The functions $f_{T,v}$ and $f_{T,j}$ for the temperature dependences of $v_{cmax,25}$ and j_{max}, respectively, were taken from Leuning (2002).

Function f_d accounts for canopy development and f_w the effect of water stress on the photosynthesis parameters. The water stress factor f_w was calculated as

$$f_w = \beta \sum_n \frac{W_{r,n}(\theta_n - \theta_{wilt})}{\theta_{fc} - \theta_{wilt}}, \quad (16)$$

where $W_{r,n}$ is the root mass fraction in soil layer n ($n = 1$–6), θ_n is volumetric soil water content of soil layer n, and θ_{wilt} and θ_{fc} are volumetric soil water content at wilting point and field capacity, respectively.

Function f_d is used to describe the influence of canopy development on v_{cmax} and j_{max} and two models for f_d are considered, viz.

Model I:

$$f_d = 1. \quad (17)$$

Model II:

$$f_d = 1 - \left(\frac{T_{s,0.5} - T_0}{\Delta T}\right)^2, \; 0 \le f_d \le 1, \quad (18)$$

where $T_{s,0.5}$ is the temperature at 0.5 m depth, T_0 and ΔT (°C) are parameters of the canopy-development model.

Both v_{cmax} and j_{max} are leaf-scale photosynthetic parameters and they are assumed to decrease exponentially with the cumulated canopy LAI from the canopy top in a canopy. Total canopy v_{cmax} and J_{max} (expressed per ground area basis) are given by

$$v_{cmax} = v_{cmax,25} f_{T,v} f_d f_w (1 - \exp(-k_n L))/k_n, \quad (19)$$

$$J_{max} = j_{max,25} f_{T,j} f_d f_w (1 - \exp(-k_n L))/k_n, \quad (20)$$

where L is canopy LAI, and k_n is an empirical constant. To compare estimates of the photosynthesis parameters derived from flux measurements at the canopy scale with those from leaf-level gas exchange measurements, we use $v_{x,25} = f_d f_w \, v_{cmax,25}$ and $j_{x,25} = f_d f_w j_{max,25}$, rather than v_{cmax} and j_{max}, because effects of leaf development and soil water stress on $v_{cmax,25}$ or j_{max} are usually not quantified in reports of leaf-level measurements. Following the notation of Wang & Leuning (1998), we use $V_{cmax,25}$ and J_{max} for the total canopy and v_{cmax} and j_{max} for the leaf within the canopy.

For given values of canopy V_{cmax} or J_{max}, the corresponding leaf $v_{cmax,25}$ or $j_{max,25}$ at the canopy top vary with k_n. The following equation can be used to calculate leaf $v_{cmax,25}$ or $j_{max,25}$ for different k_n. That is

$$v_1 = \frac{v_2 k_{n,1}(1 - \exp(-k_{n,2}L))}{k_{n,2}(1 - \exp(-k_{n,1}L))}, \quad (21)$$

where v_1 and v_2 are the value of $v_{cmax,25}$ or $j_{max,25}$ for $k_n = k_{n,1}$ and $k_n = k_{n,2}$, respectively.

The FLUXNET dataset

The goal of this study is to test a parameter optimization technique for a wide range of vegetation types growing in different climates, using measurements of heat, water vapor and CO_2 fluxes and associated meteorological variables in the gap-filled FLUXNET dataset compiled by Falge *et al*. (2001) (http://www.fluxnet.ornl.gov/fluxnet/gapzips.cfm). From the 36 sites where gap-filled data are available, eight were selected, consisting of three needle-leaved evergreen forests at high latitude, three temperate deciduous broadleaf forests, one temperate savanna, all in the northern hemisphere, and one evergreen broad-leaf forest in Australia. Information about the eight sites is given in Table 2 and the listed references.

To predict surface fluxes, F_e, F_h and F_c, CBM requires the inputs of meteorological forcing (incoming short-wave and long-wave radiation, air temperature, relative humidity, rainfall and wind speed) and four kinds of parameters: *morphological parameters*: such as canopy height, leaf size, rooting depth and vertical distribution of root mass at different soil layers, leaf angle distribution and LAI; *optical properties*: transmittance and reflectance of all phyto-elements and the ground in the visible, near infrared and long-wave wavebands; *plant physiological parameters*: $v_{cmax,25}$, $j_{max,25}$, the stomatal parameters (a and D_0), sensitivity of $v_{cmax,25}$ or $j_{max,25}$ to soil water (β), basal rate of nonleaf respiration rate at 25 °C ($r_{p,25}$); and *soil parameters*: basal rate of soil respiration at 25 °C ($r_{s,25}$), volumetric water content at wilting point and field capacity and other soil physical properties.

The most important plant morphological parameters are LAI, rooting depth and vertical distribution of roots in soil. The latter were determined for the eight selected sites using data compiled by Jackson *et al*. (1996) for boreal forests, temperate coniferous forests, temperate deciduous forests and savannas. Estimates of LAI and its seasonal variations were either derived from the literature, from MODIS products (http://public.ornl.gov/fluxnet/modis.cfm), or from site-specific websites. Canopy height and leaf size were obtained from the

Table 2 Basic information for all sites

Site	Location	Vegetation type	Period	Reference
Aberfeldy (AB)	56.6°N, 3.8°W	Evergreen conifers	1998–1999	Seibt *et al*. (2004)
Boreas (NB)	55.9°N, 98.5°W	Evergreen conifers	1995–1998	Sellers *et al*. (1997)
Hyytiala (HY)	61.9°N, 24.3°E	Evergreen conifers	1996–1998	Suni *et al*. (2003)
Harvard forest (HV)	42.5°N, 72.2°W	Broad-leaf deciduous	1992–1999	Wofsy *et al*. (1993)
Hesse (HE)	48.7°N, 7.8°E	Broad-leaf deciduous	1997–1999	Granier *et al*. (2002a)
Walker Branch (WB)	36.0°N, 84.3°W	Broad-leaf deciduous	1995–1998	Baldocchi (1997)
Tonzi (TZ)	38.4°N, 120.9°E	Oak-grass savanna	2002–1993	Baldocchi *et al*. (2004)
Tumbarumba (TB)	35.7°S, 148.2°E	Broadleaf evergreen	2002–1993	Leuning *et al*. (2005)

This study used the gap-filled flux data compiled by Fagle *et al*. (2001) which are available at http://www.fluxnet.ornl.gov/fluxnet/gapzips.cfm and data from Leuning *et al*. (2005).

published literature, internet websites or personal communication with the primary investigators. These data sources were also used for soil texture classification to estimate soil physical properties through relationships developed by Clapp & Hornberger (1978).

Estimates of optical properties for different phytoelements were taken from Wang & Leuning (1998). Leaf angle distribution is assumed to be spherical for all sites, as different leaf angle distributions were found to have relatively little influences on the modeled canopy fluxes (F_{ec}, F_{hc} and F_{cc}) and spherical leaf distribution is a good approximation for most forest canopies (see Wang & Jarvis, 1990; Baldocchi & Meyers, 1998). Effects of snow cover and snow age on surface optical properties are modeled according to Kowalczyk *et al*. (1994).

Initial soil temperature was set to annual mean temperature and initial soil moisture was set to the mean of soil moisture content at wilting point and field capacity for each layer. The model was then spun up for 5 years by reusing the same years of meteorological forcing. Soil moisture and temperature of all six layers at the end of the 5-year run were used as the initial values for the sixth year of simulations that was used for parameter estimation. Optimization results did not differ significantly from those obtained with a spin-up of >10 years.

Choosing the parameters to be optimized

Variations of $v_{cmax,25}$ and $j_{max,25}$ are the largest for different biomes (Sellers *et al*., 1996) and these parameters were estimated using PEST, with prior estimates taken from the default values in CBM for each vegetation type or from the published literature. To limit the number of parameters to be optimized, parameters for the stomatal model (Eqn (8)) were set to $a = 9$ and $D_0 = 1.5$ kPa (Leuning, 1995; Wang *et al*., 2001). The nitrogen distribution coefficient was set to $k_n = 0.7$ (Eqns (19) and (20)) for all ecosystems.

Parameter β describes the sensitivity of $v_{cmax,25}$ or $j_{max,25}$ to soil water stress (Eqn (16)). Federer (1982) discussed a similar parameter and its dependence on soil and vegetation characteristics and found that his parameter had higher values for crops and grass than for forests, because trees have deeper roots. A value of 1 was used by Colello *et al*. (1998) for their global climate simulation. The optimization did not always converge in the present study when β was allowed to vary and β ranged from 0.7 to 1.3 when the optimization did converge. We, therefore, chose $\beta = 1$ in this study.

Of the soil parameters, only basal soil respiration rate at 25 °C and optimal water condition, $r_{s,25}$, was estimated using optimization. Values of all soil physical parameters were taken from the look-up table for each soil type as used in CBM for global modeling studies (Kowalczyk *et al*., 1994).

Results

In all, six parameters are optimized in this study. They are canopy LAI (L), maximum carboxylation rate ($v_{cmax,25}$) at 25 °C of leaves at the top of the canopy, maximum potential electron transport rate at 25 °C of leaves at the top of the canopy ($j_{max,25}$), soil respiration rate at 25 °C ($r_{s,25}$) and two additional parameters, T_0 and ΔT that are used to describe the seasonal dependence of v_{cmax} or j_{max} on soil temperature at 0.5 m depth (see Eqn (17)). The prescribed canopy leaf index varies seasonally for deciduous forests and savanna, and was assumed constant for all evergreen forests. In this study, we optimized a constant multiplier of the prescribed canopy LAI, x_L. We also included the ratio $j_{max,25}/v_{cmax,25} = 2.7$ that Wullschleger (1993) and Leuning (2002) found for a wide range of plant species as prior information in the optimization. Because CO_2 fluxes for plants and soil were not measured separately, we cannot obtain independent estimates of basal rates of nonleaf plant and soil respiration ($r_{p,25}$ and $r_{s,25}$). The

Table 3 Optimal estimates of model parameters for all eight sites and different years

			μmol m^{-2} s^{-1}				°C		
Site	Year	x_L	$v_{cmax,25}$	$j_{max,25}$	$r_{s,25}$	$r_{e,25}$	T_0	ΔT	d
AB	1997	0.80 (0.02)	82.0 (1.4)	224.8 (4.4)	13.3 (0.3)	15.8	–	–	0.87
AB	1998	0.80 (0.01)	71.6 (0.9)	180.0 (3.0)	13.0 (0.3)	15.4	–	–	0.87
HY	1997	1.09 (0.01)	33.9 (0.4)	67.8 (1.0)	4.8 (0.3)	6.6	–	–	0.86
HY	1998	1.05 (0.01)	33.8 (0.4)	71.0 (1.0)	6.5 (0.3)	8.3	–	–	0.87
NB	1995	1.03 (0.01)	13.7 (0.3)	30.7 (0.3)	3.4 (0.3)	5.3	–	–	0.90
NB	1996	1.16 (0.01)	15.2 (0.1)	25.4 (0.6)	5.4 (0.3)	7.3	–	–	0.92
NB	1997	1.16 (0.01)	20.1 (0.1)	30.1 (0.7)	10.4 (0.3)	12.4	–	–	0.92
NB	1998	1.02 (0.01)	27.9 (0.3)	52.0 (0.8)	5.6 (0.3)	7.6	–	–	0.91
TB	2002	1.20 (0.01)	58.3 (0.5)	101.5 (1.1)	0.3 (0.3)	5.5	–	–	0.95
TB	2003	1.20 (0.01)	38.0 (0.2)	55.9 (1.5)	0.3 (0.3)	5.5	–	–	0.92
HE	1997	1.20 (0.03)	41.6 (1.0)	113.3 (2.9)	9.4 (0.3)	11.1	16.9 (0.1)	9.4 (0.1)	0.93
HE	1998	1.18 (0.01)	36.9 (0.6)	64.1 (1.2)	1.7 (0.3)	3.5	31.1 (0.4)	24.0 (0.5)	0.89
HE	1999	1.20 (0.01)	49.6 (1.4)	135.7 (4.0)	8.7 (0.3)	10.5	25.6 (0.8)	18.7 (1.0)	0.92
HV	1992	1.20 (0.01)	56.0 (1.7)	102.2 (3.6)	2.5 (0.3)	4.9	30.9 (1.2)	24.3 (1.3)	0.90
HV	1993	1.20 (0.01)	58.5 (1.7)	120.7 (4.0)	2.8 (0.3)	5.4	28.8 (0.9)	22.1 (1.0)	0.91
HV	1994	1.20 (0.01)	65.9 (2.3)	138.8 (5.1)	3.4 (0.3)	5.9	29.8 (1.0)	20.5 (1.0)	0.91
HV	1995	1.20 (0.01)	50.9 (2.3)	116.0 (5.3)	2.3 (0.3)	4.8	31.3 (1.4)	23.8 (1.5)	0.91
HV	1996	1.20 (0.01)	74.1 (2.3)	164.2 (5.4)	3.9 (0.3)	6.3	31.6 (0.9)	22.4 (0.9)	0.91
HV	1997	1.20 (0.01)	66.7 (2.4)	149.0 (5.5)	2.8 (0.3)	5.4	32.2 (1.1)	24.5 (1.2)	0.91
HV	1998	1.20 (0.01)	46.6 (0.4)	88.3 (0.7)	3.4 (0.3)	5.8	28.7 (0.1)	20.1 (0.1)	0.90
HV	1999	1.20 (0.01)	70.0 (2.1)	162.2 (4.8)	1.7 (0.3)	4.1	32.6 (0.8)	22.3 (0.92)	0.90
TZ	2002	1.20 (0.01)	50.1 (1.3)	105.2 (3.2)	0.3 (0.3)	1.8	32.3 (1.0)	27.8 (1.3)	0.88
TZ	2003	1.20 (0.01)	56.3 (1.3)	116.7 (3.2)	0.3 (0.3)	1.8	28.1 (1.6)	26.6 (2.6)	0.88
WB	1995	0.87 (0.01)	53.4 (0.6)	87.9 (1.2)	0.6 (0.3)	2.4	31.5 (0.2)	19.9 (0.3)	0.90
WB	1996	0.80 (0.01)	91.7 (1.5)	156.9 (3.2)	0.8 (0.3)	2.6	28.2 (0.4)	14.3 (0.4)	0.92
WB	1997	0.88 (0.01)	71.9 (0.9)	125.4 (1.9)	2.0 (0.3)	2.4	28.4 (0.4)	15.6 (0.4)	0.92
WB	1998	0.89 (0.01)	44.2 (1.1)	103.0 (2.6)	0.3 (0.3)	1.8	30.7 (0.8)	18.6 (0.9)	0.91

Where $r_{e,25} = r_{s,25} + r_{p,25}$. The Willmott (1984) agreement index, d, is dimensionless.

soil respiration parameter was thus calculated using $r_{s,25} = r_{e,25} - r_{p,25}$, where $r_{e,25}$ is total ecosystem respiration at 25 °C and $r_{p,25}$ is a fixed common prior estimate of basal plant respiration for all sites.

Table 3 lists values of all the optimized parameters in CBM with models I (Eqn (16)) or II (Eqn (17)) for seasonal variation in $v_{cmax,25}$ at the eight sites. Equivalent values of $v_{max,25}$ or $j_{max,25}$ can be computed using Eqn (20) for other value of k_n. It should be noted that the estimates of $v_{cmax,25}$ and $j_{max,25}$ depend on the temperature dependence functions ($f_{T,v}$ and $f_{T,j}$) for v_{cmax} and j_{max} and the values of the enzyme kinetic parameters and their temperature dependence (see Leuning, 2002). Values of $r_{e,25}$ listed in Table 3 represent the total ecosystem respiration rates minus leaf respiration at 25 °C and without water stress. Statistical tests (χ^2 value calculated using Eqn (4)) show that model II explains significantly more variance than model I only for the three deciduous forests (HE, HV, WB) and the savanna site (TZ). The optimization shows there was no significant seasonal variation in v_{cmax} and j_{max} for the evergreen coniferous forests and the *Eucalyptus* forest and hence no values for T_0 and ΔT_0 are presented in Table 3.

The Willmott (1984) model agreement index d exceeded 0.87 in all cases (Table 3), indicating that CBM simulates the measurements closely, but not perfectly, as this requires $d = 1$.

Table 4 lists the coefficients and r^2 values for linear regressions ($y = a + bx$) between observations (independent variable, x) and model predictions (dependent variable, y) for all site years. Values for the Wilmott agreement index are also given in Table 4. These quantities will be used to assess the agreement between model predictions and observation and any systematic bias in the model predictions.

Evergreen forests

There was no statistically significant difference between model I or II for the three evergreen forests and therefore results from CBM with model I are presented here. Figure 1 compares the predicted half-hourly values of

Table 4 Regression coefficients for $y = a + bx$, r^2 values, and the agreement index (d) for: F_e (subscript e), F_h (subscript h) or F_c (subscript c), where x are observations and y the model predictions

Site	Year	a_e	b_e	r_e^2	d_e	a_h	b_h	r_h^2	d_e	a_c	b_c	r_c^2	d_c
AB	1997	4.53	0.67	0.48	0.83	−33.01	0.69	0.53	0.82	−0.31	0.73	0.82	0.94
AB	1998	9.17	0.73	0.43	0.80	−26.69	0.84	0.66	0.88	−0.44	0.61	0.80	0.91
HY	1997	4.86	0.83	0.79	0.93	−45.60	0.54	0.68	0.74	−0.66	0.55	0.77	0.88
HY	1998	6.01	1.07	0.71	0.90	−38.21	0.82	0.74	0.84	−0.58	0.52	0.77	0.87
NB	1995	2.22	0.93	0.66	0.89	−32.84	0.72	0.80	0.89	−0.40	0.39	0.61	0.76
NB	1996	1.02	0.91	0.70	0.91	−33.53	0.77	0.80	0.90	−0.15	0.40	0.63	0.78
NB	1997	1.81	0.93	0.67	0.90	−39.80	0.73	0.76	0.86	−0.10	0.46	0.68	0.82
NB	1998	1.97	0.65	0.72	0.89	−35.23	0.72	0.74	0.86	−0.12	0.45	0.60	0.81
TB	2002	7.82	0.99	0.80	0.94	−16.46	0.86	0.84	0.95	−0.58	0.68	0.79	0.92
TB	2003	6.54	1.00	0.73	0.92	−8.97	0.82	0.84	0.95	−0.44	0.52	0.66	0.85
HE	1997	5.70	0.62	0.48	0.76	−8.48	1.16	0.70	0.00	−0.16	0.78	0.76	0.93
HE	1998	7.14	1.10	0.75	0.91	−8.81	0.87	0.67	0.90	−0.92	0.39	0.63	0.78
HE	1999	9.24	1.09	0.77	0.92	−8.84	0.89	0.72	0.91	−0.29	0.62	0.71	0.89
HV	1992	1.04	0.90	0.75	0.90	−6.33	0.38	0.33	0.71	−0.48	0.77	0.75	0.92
HV	1993	1.33	0.95	0.78	0.92	−11.00	0.38	0.32	0.70	−0.79	0.74	0.77	0.92
HV	1994	6.39	1.04	0.77	0.89	−9.16	0.31	0.28	0.66	−0.55	0.77	0.79	0.93
HV	1995	8.07	1.04	0.77	0.90	−4.92	0.32	0.30	0.67	−0.61	0.76	0.81	0.93
HV	1996	5.60	1.03	0.79	0.91	−9.26	0.39	0.40	0.73	−0.53	0.75	0.78	0.93
HV	1997	6.09	1.06	0.74	0.89	−4.09	0.35	0.35	0.70	−0.76	0.72	0.78	0.92
HV	1998	3.34	1.03	0.74	0.89	−9.64	0.38	0.37	0.70	−0.39	0.70	0.73	0.91
HV	1999	5.00	1.04	0.76	0.90	−7.59	0.30	0.32	0.66	−0.56	0.74	0.76	0.92
HY	1997	6.65	0.90	0.83	0.94	−45.32	0.55	0.69	0.74	−0.26	0.64	0.80	0.91
HY	1998	7.35	1.10	0.76	0.91	−37.60	0.86	0.76	0.85	−0.00	0.68	0.79	0.92
TZ	2002	7.00	1.34	0.62	0.82	10.87	0.88	0.82	0.95	−0.19	0.40	0.49	0.76
TZ	2003	6.21	1.21	0.60	0.83	8.53	0.87	0.82	0.95	−0.62	0.40	0.45	0.75
WB	1995	0.29	1.04	0.69	0.89	−14.94	1.13	0.68	0.87	−0.50	0.64	0.63	0.88
WB	1996	4.81	1.14	0.78	0.92	−12.75	1.09	0.65	0.87	−0.38	0.85	0.79	0.94
WB	1997	4.80	1.02	0.76	0.92	−14.39	0.98	0.66	0.88	−0.41	0.80	0.76	0.93
WB	1998	1.95	1.07	0.70	0.89	−13.12	0.96	0.64	0.88	−0.68	−0.68	0.72	0.90

All quantities are dimensionless.

F_e, F_h and F_c for two temperate evergreen forests, one coniferous (AB), the other a broad leafed *Eucalyptus* forest (TB). The model simulates all three fluxes quite well on average. Table 4 shows there is little bias in model predictions of F_e and that the slopes of the linear regressions are close to unity for site TB. The model also accounts for a high proportion of the observed variance in F_e, as shown by the high r^2 values and by the agreement index, d. CBM significantly underestimated F_h for the AB site and to a lesser degree at TB, with regression slopes <0.9 and biases of $-30\,W\,m^{-2}$ for AB and $15\,W\,m^{-2}$ for TB. The systematic underestimation of F_h is seen more clearly in the time series of monthly average fluxes for AB in Fig. 2 and for TB in Fig. 3. For CO_2 fluxes, there was good agreement between model predictions and measurements when F_c was $>-15\,\mu mol\,m^{-2}\,s^{-1}$ but the model was unable to simulate net CO_2 fluxes when F_c was more negative for both the AB and TB sites (Figs 1–3). The simulated mean F_c is more positive than was observed for April and May in both years for site AB (Fig. 2) and for the Austral summers for site TB (Fig. 3).

An independent study of carbon fluxes at site TB showed that the year 2002 was much wetter than 2003 and therefore annual net CO_2 uptake was also much larger (Leuning *et al*., 2005). The observed annual net CO_2 uptake was $988\,g\,C\,m^{-2}\,yr^{-1}$ in 2002 and $364\,g\,C\,m^{-2}\,yr^{-1}$ in 2003, compared with the predicted totals of 890 and $359\,g\,C\,m^{-2}\,yr^{-1}$ for 2002 and 2003, respectively. The model is able to reproduce the large inter-annual variations of F_c between year 2002 and 2003 for site TB only by reducing $v_{cmax,25}$ by 33% and $j_{max,25}$ by 44% in 2003 relative to 2002. This may be an artifact of keeping LAI constant in the optimization, as there was significant defoliation associated with the drought and an insect attack on the forest in 2003.

The optimization showed no significant seasonal variations of $v_{cmax,25}$ and $j_{max,25}$ for the evergreen forests, so the development function, $f_d = 1$ and $v_{x,25} = v_{cmax,25}$ and $j_{x,25} = j_{max,25}$ when water stress also

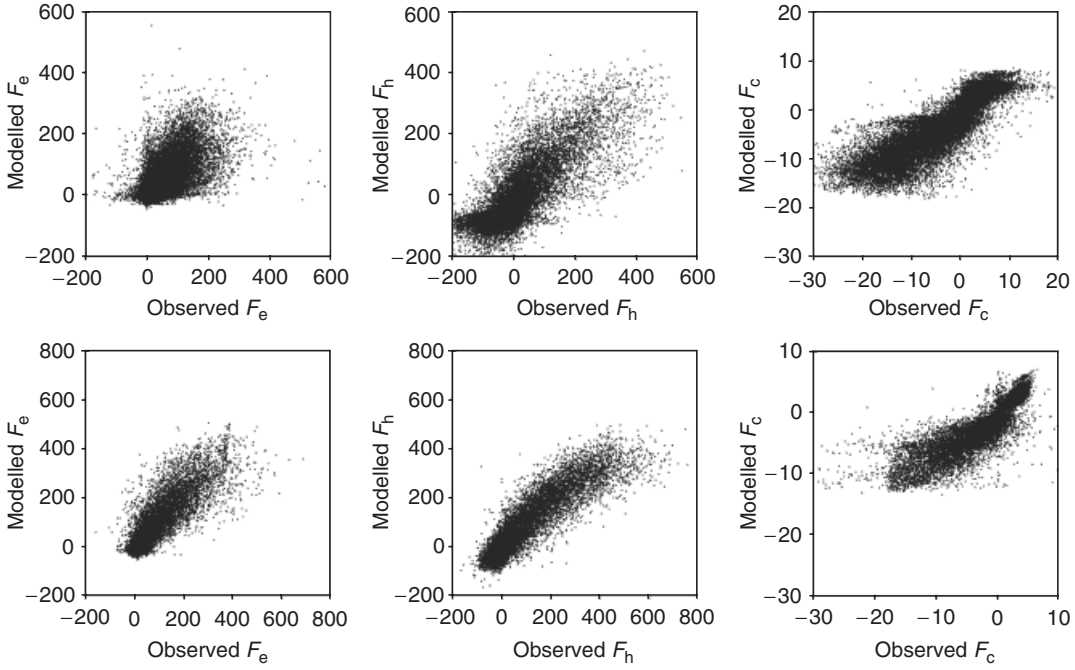

Fig. 1 Comparison of the observed and modeled F_e, F_h and F_c for site AB (upper three panels) or TB (lower three panels). The units are W m^{-2} for F_e and F_h, and μmol m^{-2} s^{-1} for F_c.

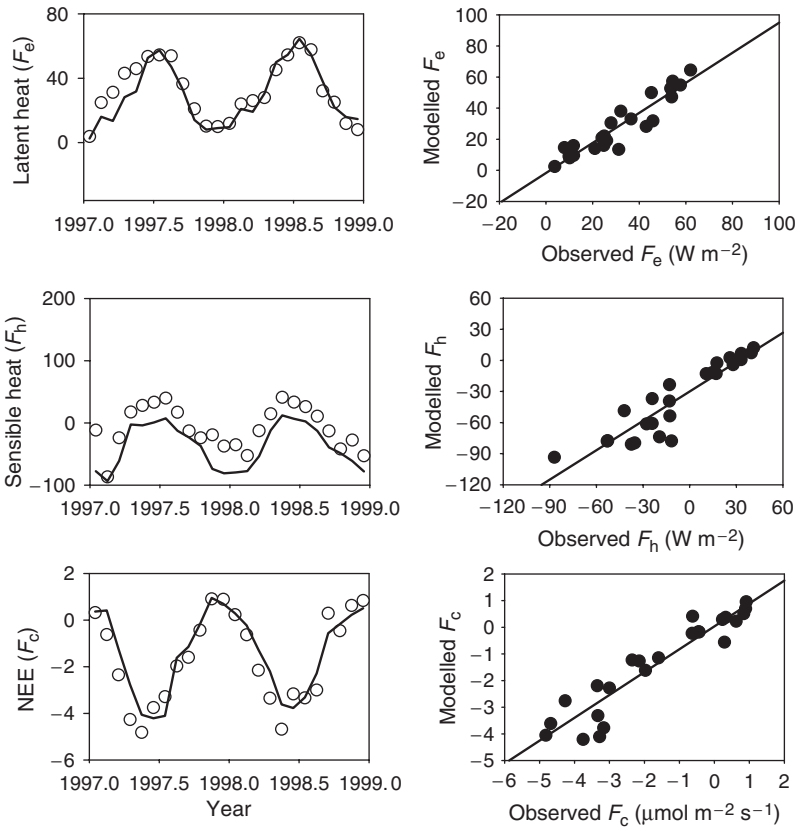

Fig. 2 Left-hand panels: monthly mean fluxes of F_e, F_h and F_c for site AB as observed (○) and predicted by CSIRO biosphere model (line). Right-hand panels: scatter plots of modeled vs. observed monthly mean fluxes with regression lines (Table 4).

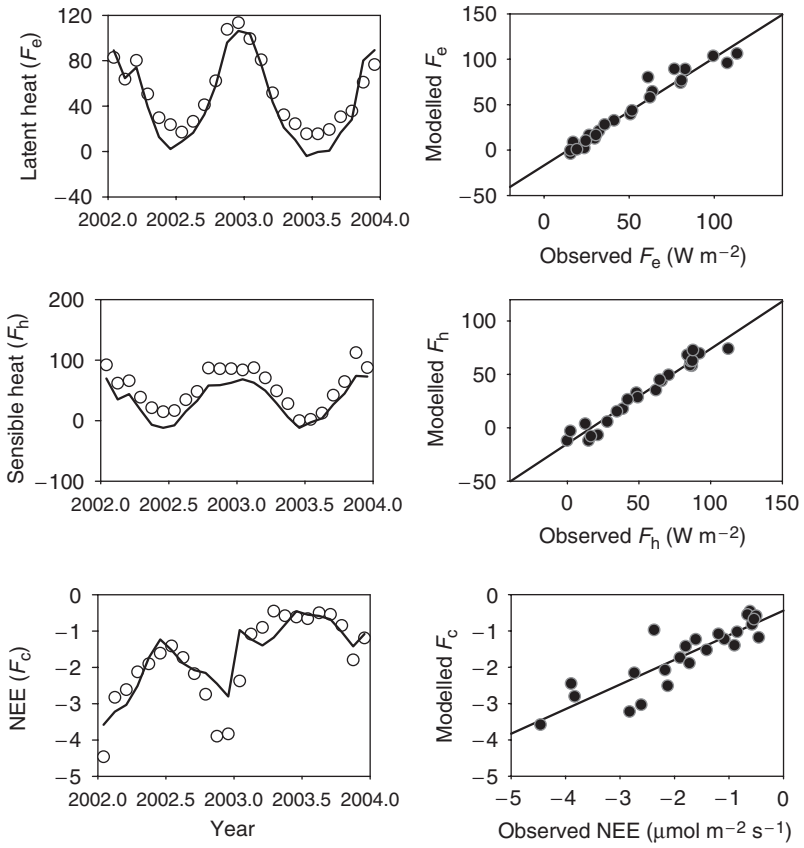

Fig. 3 Left-hand panels: monthly mean fluxes of F_e, F_h and F_c for site TB as observed (○) and predicted by CSIRO biosphere model (line). Right-hand panels: scatter plots of modeled vs. observed monthly mean fluxes with regression lines (Table 4).

is absent (Eqns (19) and (20)). Using leaf-gas exchange measurements, Meir *et al*. (2002) estimated that $v_{cmax,25}$ varied from 40 to 20 μmol m^{-2} s^{-1} from the top to the bottom of a Sitka Spruce forest near the AB site. Their results agree well with our estimates if $k_n = 0.35$ (assuming a canopy LAI of 7 and applying Eqn (20)). Maximum canopy photosynthesis occurs when the vertical distribution of photosynthetic capacity in the canopy in proportional to average radiation absorption at each height (Field, 1983; de Pury & Farquhar, 1997; Wang & Leuning, 1998). The low value of k_n is thus possible, as Wang & Jarvis (1993) estimated that the effective extinction coefficient of diffuse visible radiation within a dense Sitka spruce canopy is about 0.4 because of needle clumping. For the TB site in 2002, leaf gas exchange measurements on leaves in the middle part of the forest canopy gave a mean value for $v_{cmax,25}$ of 84 μmol m^{-2} s^{-1} (B. E. Medlyn, unpublished data), which is about twice our estimates for $k_n = 0.7$. It is unlikely that the estimate of k_n will exceed 0.7 for site TB, as the canopy is quite open with a maximal canopy LAI of 2.5 (Leuning *et al*., 2005) and hence the reason for the discrepancy is as yet unclear.

No significant seasonal variations in $v_{cmax,25}$ and $j_{max,25}$ was required for CBM for two high-latitude, evergreen boreal forest sites, HY and NB (results not shown), in contrast to Wang *et al*. (2003) who found a significant seasonal variation in $v_{cmax,25}$ at site HY. These contrasting results may arise from the use of different functions to describe the temperature dependences of v_{cmax} and j_{max}. As with the AB and TB sites, CBM predicts the monthly F_e throughout the year and F_c during the growing season quite well for the HY and NB sites, but systematically underestimates the sensible heat fluxes at all times. Systematic model errors in F_h can arise if CBM overestimates surface albedo, underestimates the net available energy, or if CBM underestimates aerodynamic resistance in the canopy (Baldocchi & Harley, 1995).

Estimates of $v_{cmax,25} = 34$ μmol m^{-2} s^{-1} and $j_{max,25} = 69$ μmol m^{-2} s^{-1} for $k_n = 0.7$ at the site HY in 1997 and 1998 are 40% and 23% lower, respectively, than the corresponding values estimated by Aalto (1998) from field gas exchange measurements. These differences may result from the different functions used by Aalto (1998) to describe the temperature dependences

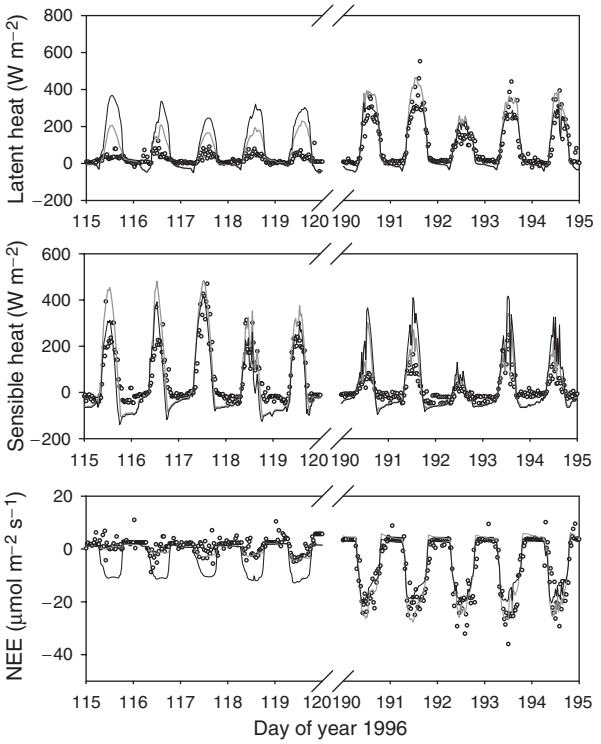

Fig. 4 Half-hourly fluxes of F_e, F_h and F_c at site WB as observed (○) or predicted using CSIRO biosphere model with model I (black curve) or model II (dark grey curve) for v_{cmax} and j_{max} at the beginning (DOY 115–120) or peak (190–195) growing season in 1996.

of v_{cmax} and j_{max}, and the possible invalidity of the assumption that both v_{cmax} and j_{max} decline exponentially with the cumulative canopy LAI from the canopy top.

Values of $v_{cmax,25}$ at site NB obtained from CBM with $k_n = 0.7$ agreed well with those for needles in the upper canopy in July obtained by Rayment *et al*. (2002) from field gas exchange measurements and by Dang *et al*. (1998). The optimization suggests that there are no strong seasonal trends in $v_{cmax,25}$ and $j_{max,25}$ at NB, which is consistent with Dang *et al*. (1998), but contrary to the findings of Rayment *et al*. (2002). Because winter temperature at NB can be as low as $-30\,^{\circ}C$, v_{cmax} and j_{max} would be close to 0 during winter time, our results suggest that temperature adaptation of photosynthetic machinery is rather weak at NB during the growing season.

Deciduous forests

Photosynthetic capacity changes during leaf development and senescence (Wilson *et al*., 2001; Tanaka *et al*., 2002; Xu & Baldocchi, 2003) and this physiological change is more evident in deciduous than in evergreen forests (Gill *et al*., 1998). Comparison of modeled and measured half-hourly fluxes in Fig. 4 shows that CBM with constant $v_{x,25}$ (Model I) overestimates the magnitudes of F_e and F_c at the beginning of the growing season at the WB site, and underestimates these fluxes in the middle of growing season, a result also found by Wilson *et al*. (2001). Significantly better agreement between predicted and observed monthly averaged F_e, F_h and F_c are obtained if Model II is used to describe seasonal variation in $v_{x,25}$ and $j_{x,25}$ at WB (Fig. 5), as well as at the other two deciduous forest sites (HE, HV) and at the oak savanna (TZ) (data not shown). CBM predicts a negative F_e over the winter months, whereas the measurements show a small but positive F_e (Fig. 5). As with other sites, there is poor agreement between the observed and predicted F_h, e.g. the predicted F_h during winter months of 1996 at WB are negative while the observed F_h always are positive (i.e. see also Table 4).

Our estimates of ecosystem respiration rate for site HE varies from $3.5\,\mu mol\,m^{-2}\,s^{-1}$ in 1998 to $11.0\,\mu mol\,m^{-2}\,s^{-1}$ in 1997 and 1999 at $25\,^{\circ}C$ excluding leaves, the estimated rates are $7.9\,\mu mol\,m^{-2}\,s^{-1}$ for plant respiration rate including leaves and $12.7\,\mu mol\,m^{-2}\,s^{-1}$ for soil respiration (including roots) at $25\,^{\circ}C$ after correcting for temperature difference using Eqns (9) and (12) (Granier *et al*., 2002a, b).

Seasonal trends in $v_{x,25}$ obtained by optimizing CBM using flux measurements are in good agreement with $v_{x,25}$ derived from leaf gas exchange measurements on major tree species at WB by Wilson *et al*. (2001) in 1998, but are greater than leaf-level values for 1997 (Fig. 6). The leaf-level maximum in $v_{x,25}$ occurs during April and May, whereas CBM predicts a maximum in July. These differences may arise from small errors in the prescribed LAI. Water stress during the growing season has significant impact on canopy photosynthetic capacity according to CBM, as shown by the considerably lower values of $v_{x,25}$ and $j_{x,25}$ during the relatively dry 1995 and 1998 growing seasons (Fig. 6, Table 3), corresponding to lower canopy leaf area indices, and smaller water vapor and CO_2 fluxes compared with 1996 and 1997 during July and August (Fig. 5, Baldocchi, 1997). Law *et al*. (2002), Oechel *et al*. (2000), Wilson & Baldocchi (2000), Leuning *et al*. (2005) and many others have shown that mean annual temperature and soil water availability strongly affect interannual variations in gross photosynthesis and net carbon balance and part of this variation may be due to photosynthetic capacity. While there is a strong seasonal fluctuation in $v_{x,25}$ and $j_{x,25}$, interannual variations of the estimated $v_{x,25}$ and $j_{x,25}$ at the WB and HV site were rather small, with the coefficient of variation $<20\%$ (Figs 6 and 7).

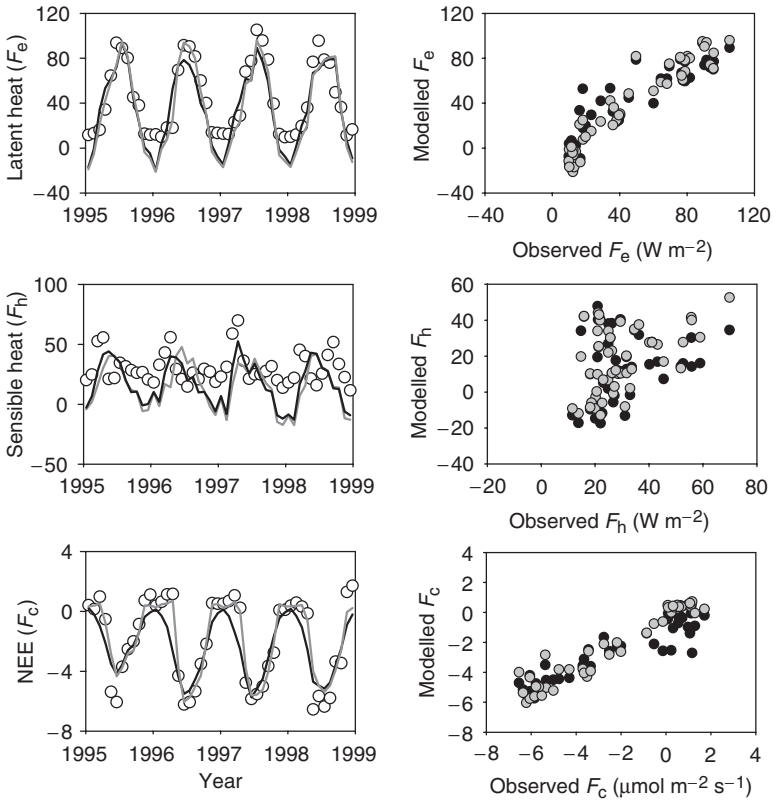

Fig. 5 Left-hand panels: monthly mean fluxes of F_e, F_h and F_c at site WB as observed (○) and predicted by CSIRO biosphere model (CBM) with model I (black curve) or model II (grey curve) for $v_{x,25}$ and $j_{x,25}$. Right-hand panels: comparison of the observed and predicted monthly mean fluxes using CBM with model I (●) or model II (grey circle) for $v_{x,25}$ and $j_{x,25}$.

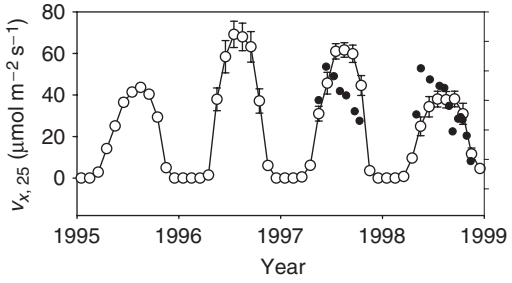

Fig. 6 Comparison of the seasonal variation of $v_{x,25}$ for site WB estimated using nonlinear optimization of CSIRO biosphere model (line with ○) with estimates of $v_{x,25}$ derived from leaf gas exchange measurements by Wilson *et al*. (2001) (●).

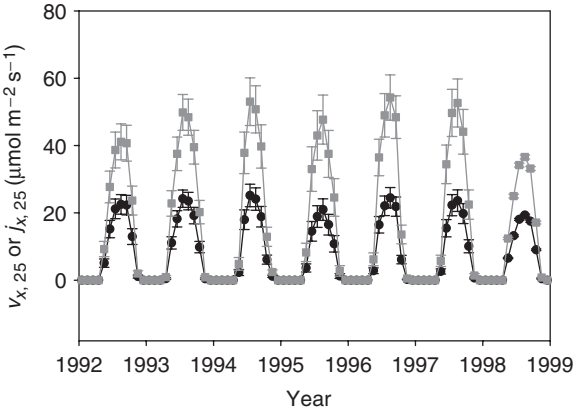

Fig. 7 Variations of optimal estimates of $v_{x,25}$ (black) or $j_{x,25}$ (grey) of a deciduous forest at site HV from 1992 to 1999. The error bar represents ± 1 standard deviation.

Model II for $v_{\max,25}$ and $j_{\max,25}$ in CBM improved the agreement between the predicted and the observed fluxes for all three fluxes at site HV from 1992 to 1999 but even after optimization, the statistical analysis in Table 4 suggests that CBM underestimates F_e and F_h throughout the year for the period 1992–1999. Detailed analysis also showed that CBM also underestimates respiration during winter time, but predicted F_c during growing seasons very well. Our estimates for $v_{\mathrm{cmax},25}$ vary from 47 to 74 μmol m^{-2} s^{-1} and 88 to 164 μmol m^{-2} s^{-1} for $j_{\max,25}$ after correcting for LAI (see Table 3), which agree well with the estimates from field measurements by Bassow & Bazzaz (1997), but are significantly lower than the values used in a simulation study for Harvard Forest by Williams *et al*. (1996).

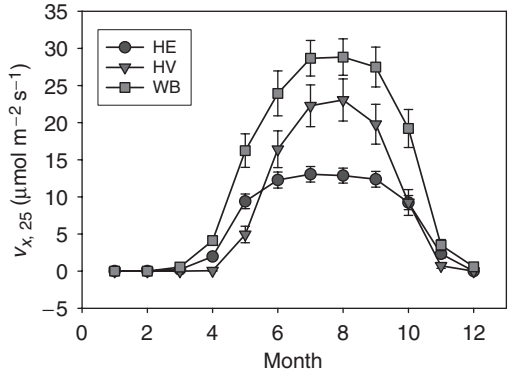

Fig. 8 Seasonal variations of $v_{x,25}$ for three deciduous forests at site HE, HV and WB when soil water stress is absent ($f_w = 0$).

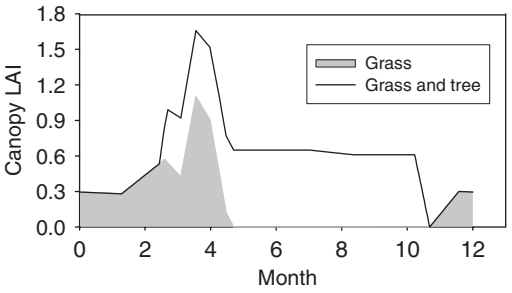

Fig. 9 Variations of leaf area indices of grasses or grasses and trees for site TZ as estimated by optimization ($\alpha_L = 1.2$). The shaded grey area represents the leaf area index (LAI) of the grass canopy and the white gap between the black curve and grey area represents the LAI of oak trees.

The seasonal variations of v_{cmax} or j_{max} for deciduous forests depend on leaf phenology and this is usually modeled using accumulated day-degrees, with a chilling requirement for some species (Kramer *et al*., 2000). In CBM, this dependency is modeled as a function of soil temperature rather than air temperature, this is consistent with the finding by Baldocchi *et al*. (2005). Soil has a significant heat capacity and hence the amplitude of the soil temperature wave decreases with soil depth while the time lag between peak soil and air temperature increases with depth. Soil temperature at depth can, thus, be used as a surrogate for accumulated day degrees of air temperature. Figure 8 shows that both the amplitude and timing of the seasonal variation of $v_{x,25}$ associated with the onset of leaf growth differ among the three deciduous forests (Xu & Baldocchi, 2003). Variation among three different deciduous sites largely results from the difference in climate, as the mean and standard deviation of the estimated T_0 are 29.3 and 3.7 °C, respectively, for different sites and different years. Two parameters, T_0 and ΔT (Eqn (18)), are used to distinguish between the various sites (Table 3). Dependence of maximum photosynthetic rates on leaf phenology was considered by Pelkonen & Hari (1980) in modeling the recovery of photosynthesis in the spring time, but so far has not been adopted by any land-surface models for global applications.

Savanna

The savanna canopy at site TZ consists of two layers of canopy: oak trees and grassland underneath. Oak trees are deciduous, their LAI increases during spring when buds break and leaves grow, and reaches a steady value of 0.6 from May to October, and then falls to 0 in November, whereas the grass understorey maintains a steady LAI during winter time (about 0.3), and dies during summer drought from May to October (Fig. 9; Baldocchi *et al*., 2004). Choice of model I or II for the seasonal variation in v_{cmax} and j_{max} (Eqns (17) and (18)) had no effect on the monthly mean F_e or F_h predicted by CBM, but F_c with model II agrees with the observations significantly better than with model I at 95% confidence interval (Fig. 10). Although most of the monthly variation of F_c is explained by LAI dynamics, CBM with a constant $v_{x,25}$ predicts a more negative F_c during the peak growing season in April and May of 2003, before the onset of summer water stress from June to October (Fig. 10). Gas exchange measurements on the leaves of overstorey oak trees showed a strong seasonal variation of $v_{x,25}$ during the growing season of 2001 (Xu & Baldocchi, 2003), being maximal in May and decreasing gradually over the summer from June to August. This trend is consistent with the estimates of $v_{x,25}$ for both trees and grasses in the savanna ecosystem for years 2002 and 2003 when effects of water stress on photosynthesis are included (Fig. 11). Estimates from CBM of seasonal $v_{x,25}$ for 2002 and 2003 are significantly lower than those obtained by leaf gas exchange measurements for the overstorey oak trees in 2001 by Xu & Baldocchi (2003). These differences may result from different scales by which two measurements represent. Fluxes measured by eddy covariance represent the mean fluxes near the flux towers in the prevailing wind direction. Only 40% of the ground area is covered by oak trees, and remaining ground surface was covered by grasses, whereas leaf gas exchange measured as reported by Xu & Baldocchi (2003) are for oak tree leaves only. The reduction in $v_{x,25}$ from May to September from the optimization of CBM resulted from the effect of water stress on the overstorey oak trees, as soil temperature was no longer a significant limiting factor after June (Fig. 11).

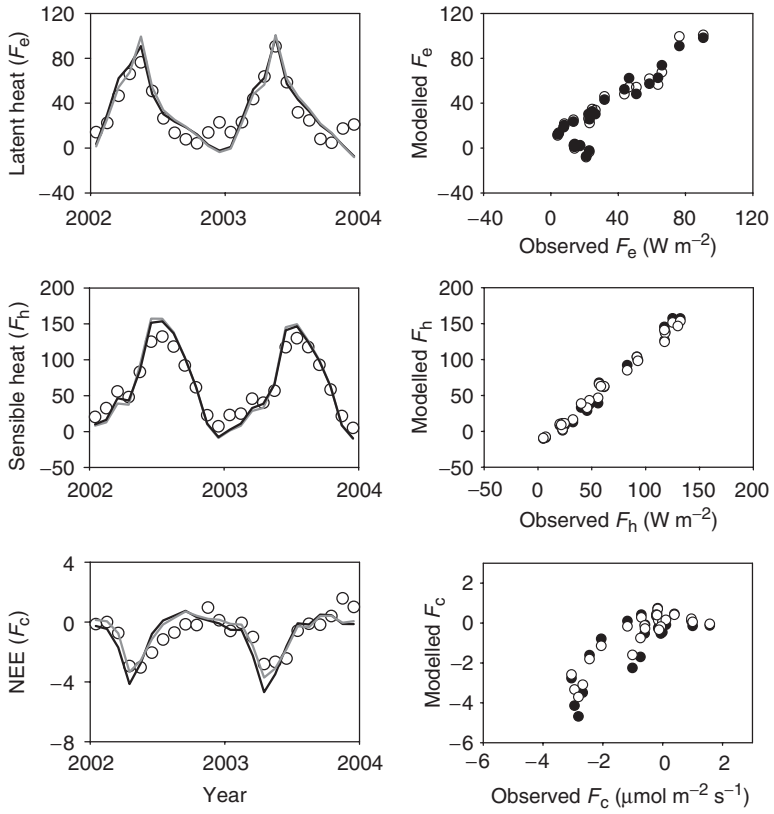

Fig. 10 Left-hand panels: monthly mean fluxes of F_e, F_h and F_c at site TZ as observed (○) and predicted by CSIRO biosphere model (CBM) with model I (black curve) or model II (grey curve) for $v_{x,25}$ and $j_{x,25}$. Right-hand panels: comparison of the observed and predicted monthly mean fluxes using CBM with model I (black circle) or model II (grey circle) for $v_{x,25}$ and $j_{x,25}$.

Photosynthesis of oak-grass savanna at TZ was clearly affected by short-term variation of leaf temperature and incoming solar radiation, and seasonal variation of water stress and leaf development (Fig. 11). Short-term variation of the environment experienced by the canopy resulted in rapid fluctuations in the fluxes of energy and net ecosystem exchange, while the seasonal variation of water stress and leaf development resulted in maximal carbon uptake and water flux during April and a minimum in November (Fig. 10). These seasonal variations at the savanna at TZ are significantly different from other forests studied, where maximal CO_2 uptake usually occur in summer.

Model errors

Systematic model errors can be identified by comparing model predictions with field measurements. Model errors can result from incorrect parameter values, deficiencies in model formulation or structure, or both. Systematic model errors can also affect the interpretation of parameter statistics (correlation and standard deviation) as we assumed that the residual errors are normally distributed.

Agreement between model predictions and observations is better for F_c and F_e than for F_h for all the eight sites studied (Table 4). Relative uncertainties in the observed fluxes are generally larger at night than during the day (Moncrieff *et al*., 1996) and thus the mean difference between model predictions and observations for day time and night time were calculated separately (Figs 12 and 13). For all eight sites, the average daytime F_c from CBM is $\sim 1\,\mu mol\,m^{-2}\,s^{-1}$ more positive than the observations but predicted F_c is more negative then the observations at night. The mean differences in F_c are less than $1\,\mu mol\,m^{-2}\,s^{-1}$ except for night time at HE (1998) and at HV, where the model underestimates night-time F_c by 1–2 $\mu mol\,m^{-2}\,s^{-1}$ (Fig. 13).

Systematic biases in the predicted F_e are rather small and positive for most site years during day time ($<16\,W\,m^{-2}$), and small ($<20\,W\,m^{-2}$) but consistently negative during night time for all eight sites except the savanna site (TZ, Fig. 12). The biases in the predicted F_e for site TZ are quite large, with means of $39\,W\,m^{-2}$

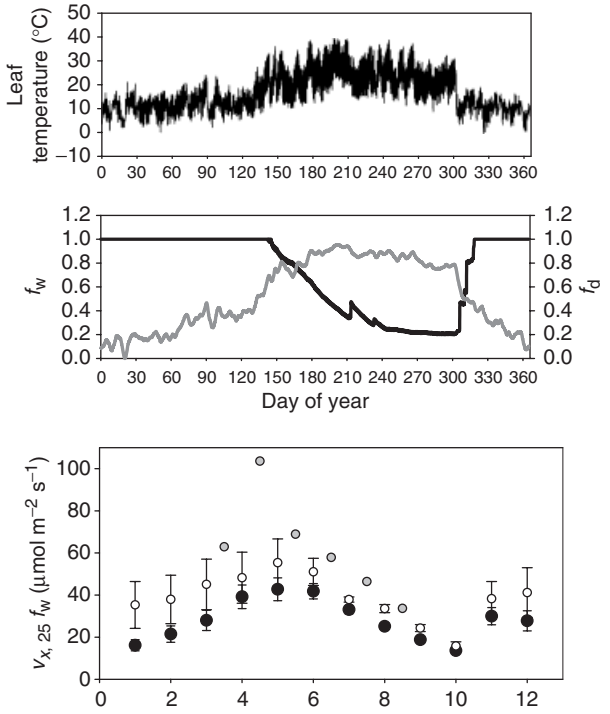

Fig. 11 Upper panel: variation of hourly canopy temperature. Middle panel: variation of daily water stress (f_w) and soil temperature on leaf development (f_d) as used in modeling canopy photosynthesis. Lower panel: comparison of the estimates of $f_w v_{x,25}$ from optimization of CSIRO biosphere model for year 2002 (•), year 2003 (○) and estimates from field gas exchange measurements in 2001 (filled grey circle) by Xu & Baldocchi (2003).

for the day time and $-38\,W\,m^{-2}$ during night-time, resulting in only small net bias over 24 h. Biases in the predicted F_e are negative for both day and night at HV, suggesting that the model underestimates the net radiation at that site.

The model underestimates mean F_h by 6–64 $W\,m^{-2}$ for evergreen forests during daytime and 5–39 $W\,m^{-2}$ during night-time for the four evergreen forests and the savanna site. Systematic biases in the predicted F_h are quite small for site HE and WB for both day time and night-time, but at site HV the model consistently underestimates F_h by 57–78 $W\,m^{-2}$ during daytime, but the biases are small ($<10\,W\,m^{-2}$) at night. Significant underestimation of F_h by CBM may result from incorrect calculation of net radiation due to overestimation of canopy albedo or underestimation of incoming longwave radiation, or the inadequate representation of canopy turbulence in our model and some other land-surface models, as demonstrated by Baldocchi (1992) and Baldocchi & Harley (1995). A study by Hanan *et al.* (2005) also found that SiB2 overestimated ground heat fluxes and underestimated sensible heat fluxes for a grassland and a wheat crop, but that the net radiation predicted by SiB2 agreed quite well with measurements. The systematic biases in CBM predictions and their implications in climate predictions by a global climate model with our land-surface model are being investigated (Abramowitz *et al.*, 2005).

Conclusions

Process-based terrestrial ecosystem models have now been used in global climate modeling and atmospheric inversion studies (Kaminski *et al.*, 2002). Global vegetation in these models is typically classified by biome, and look-up tables are used estimate model parameters for each biome (e.g. Sellers *et al.*, 1996). The parameters have generally been derived from small numbers of measurements at the plant scale or from expert judgment. However, parameters determined at one scale lead to incorrect predictions at other scales if there is a nonlinear relationship between model parameters and predicted fluxes. To overcome this problem at the 100–1000 m scale, six key parameters in the CBM were estimated in this study by applying a nonlinear inversion technique to measurements of fluxes of heat, water vapor and carbon dioxide for eight forest ecosystems. Estimates of two photosynthetic parameters, $v_{cmax,25}$, $j_{max,25}$ at the canopy scale were somewhat lower than from leaf gas exchange measurements for an evergreen broad-leaved forest, oak-grass savanna and two high latitude evergreen forest. Good agreement was found for a boreal forest and deciduous forests. More importantly, $v_{x,25}$ and $j_{x,25}$ were found to vary seasonally as leaves develop for the deciduous forests studied. To our knowledge, seasonal variations of $v_{x,25}$ and $j_{x,25}$ have not been taken into account in any land-surface schemes used in global climate modeling so far. This may result in systematic bias in the modeled net carbon fluxes from deciduous forests and predicted seasonal variation of atmospheric CO_2 concentration over the land surface in the mid-latitudes region. Most global inversions so far have not considered systematic model errors separately from measurement errors, any bias in model predictions will result in bias in the inversion estimates.

The CBM was able to simulate water vapor and CO_2 fluxes quite well, with small systematic and random error (Table 4, Figs 12 and 13). However, CBM systematically underestimated the sensible heat flux for most of the eight sites studied, even after optimizing six key model parameters using measured fluxes. This implies that there may be some structural deficiencies in the model, possibly in the calculated albedos or net radia-

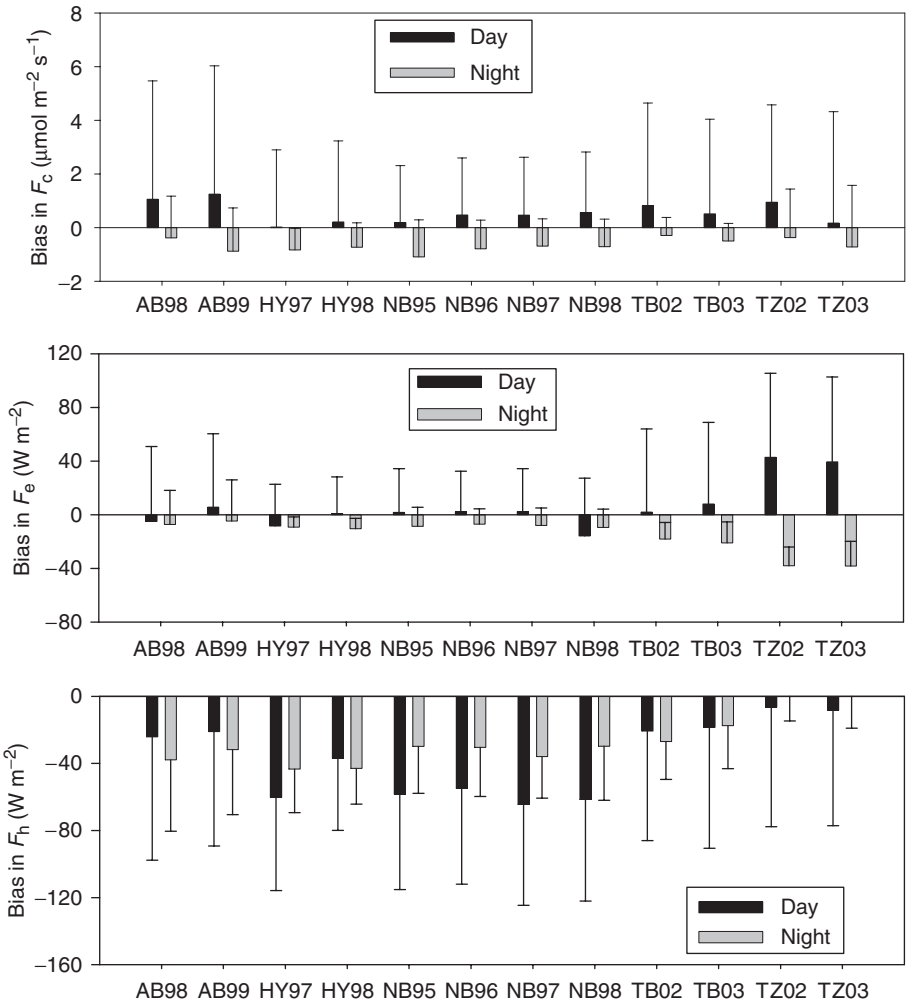

Fig. 12 Mean and 1 standard deviation of systematic biases (prediction−observation) in F_c, F_e and F_h for all evergreen forests and savanna site.

tion, or that the default values used for the fixed model parameters were incorrect. These are being actively investigated (Abramowitz *et al*., 2005).

Global land-surface models have evolved from simple tipping-bucket models to the fully interactive models (Pitman, 2003). Sustained effort has also been made in comparing different land-surface models with field observations (Chen *et al*., 1997; Pitman *et al*., 1999; and references at http://www.cic.mq.edu.au/pilps-rice/). In the development of global land-surface models, one of the major difficulties is to ensure that the models are applicable to a wide range of terrestrial ecosystems, ranging from desert to arctic biomes, under the present and future climate conditions. Past validation of model predictions was limited by field observations. With the establishment of growing number of surface flux towers and flux-tower-related studies, we need to establish a systematic framework for calibrating and validating different land-surface models, therefore, field measurements can be used to improve the parameterization or identification of systematic errors resulting from model structure or formulation. This study is a step in that direction. The framework developed here can also be used for other land-surface models because the optimization framework using PEST is independent of land-surface models and their structure and all site-specific information is contained in one input file. This study contributes to the applications of nonlinear optimization in improving the predictions of global land-surface models.

Acknowledgements

We thank the Australian Greenhouse Office and the Australian Academy of Sciences for their support of this work. Part of this work was completed while the senior author was visiting to University of California, Berkeley and Carnegie Institution of Washington, Stanford. We are grateful for the tremendous

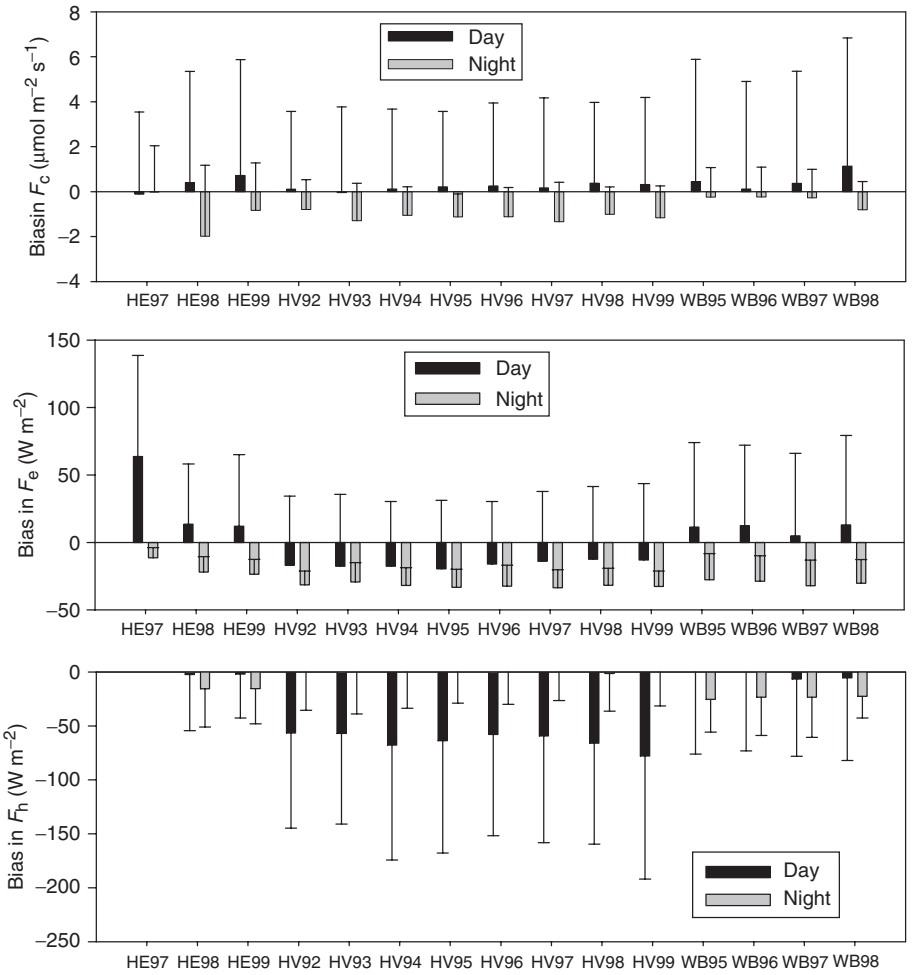

Fig. 13 Mean and 1 standard deviation of systematic biases (prediction−observation) in F_c, F_e and F_h for deciduous forests.

amount of efforts of all scientists involved in collecting and analyzing the flux data used in this study, and the establishment of AmeriFlux, Fluxnet, Ozflux, CarboEurope and the financial support of research at Hyytiala by the Academy of Finland. We thank Professor Steve Wofsy of Harvard University for making their estimates of canopy LAI and other information of the Harvard forests available to us and Dr M. Falk of the University of California for sharing his insight about the sites and measurements with us. We also thank Drs Cathy Trudinger and Bernard Pak for their constructive comments.

References

Aalto T (1998) Carbon dioxide exchange of Scots pine shoots as estimated by a biochemical model and curvette field measurements. *Silva Fennica*, **32**, 321–336.

Aalto T, Ciais P, Chevillard A *et al*. (2004) Optimal determination of the parameters controlling biospheric CO_2 fluxes over Europe using eddy covariance fluxes and satellite NDVI measurements. *Tellus*, **56B**, 93–104.

Abramowitz G, Gupta H, Pitman A *et al*. (2005) Neural error regression diagnosis (NERD): a tool for model bias identification and prognostic data assimilation. *Journal of Hydrometeorology*, **7**, 160–177

Baldocchi DD (1992) A Lagrangian random walk model for simulating water vapor, CO_2, and sensible heat flux densities and scalar profiles over and within a soybean canopy. *Boundary Layer Meteorology*, **61**, 113–144.

Baldocchi DD (1997) Measuring and modeling carbon dioxide and water vapor exchange over a temperate broad-leafed forest during the 1995 summer drought. *Plant, Cell and Environment*, **20**, 1108–1122.

Baldocchi DD, Black TA, Curtis PS *et al*. (2005) Predicting the onset of net carbon uptake by deciduous forests with soil temperature and climate data: a synthesis of FLUXNET data. *International Journal of Biometeorology*, **49**, 377–387 doi: 10.1007/s00484-005-0256-4.

Baldocchi DD, Falge E, Gu LH *et al*. (2001) FLUXNET: a new tool to study the temporal and spatial variability of ecosystem-scale carbon dioxide, water vapor, and energy flux densities. *Bulletin of the American Meteorological Society*, **82**, 2415–2434.

Baldocchi DD, Harley PC (1995) Scaling carbon dioxide and water vapor exchange from leaf to canopy in a deciduous forest: model testing and application. *Plant, Cell and Environment*, **18**, 1157–1173.

Baldocchi DD, Meyers TP (1998) On using eco-physiological, micrometeorological and biogeochemical theory to evaluate

carbon dioxide, water vapor and gaseous deposition fluxes over vegetation. *Agricultural and Forest Meteorology*, **90**, 1–26.

Baldocchi DD, Xu LK, Kiang N (2004) How plant functional-type, weather, seasonal drought, and soil physical properties alter water and energy fluxes of an oak-grass savanna and an annual grassland. *Agricultural and Forest Meteorology*, **123**, 13–39.

Bassow SL, Bazzaz FA (1997) Intra- and inter-specific variation in canopy photosynthesis in a mixed deciduous forest. *Oecologia*, **109**, 507–515.

Black TA, Den Hartog G, Neumann H *et al*. (1996) Annual cycle of water vapour and carbon dioxide fluxes in and above a boreal aspen forest. *Global Change Biology*, **2**, 219–229.

Braswell B, Sacks WJ, Linder E *et al*. (2005) Estimating diurnal to annual ecosystem parameters by synthesis of a carbon flux model with eddy covariance net ecosystem exchange observations. *Global Change Biology*, **11**, 335–355.

Chen TH, Henderson-Sellers A, Milley PCD *et al*. (1997) Cabauw experiment results from the Project for Intercomparison of Land Surface parameterization Schemes. *Journal of Climate*, **10**, 1194–1215.

Clapp RB, Hornberger GM (1978) Empirical equations for soil hydraulic properties. *Water Resources Research*, **14**, 601–604.

Colello GD, Grivet C, Sellers PS *et al*. (1998) Modeling of energy, water, and CO_2 flux in a temperate grassland ecosystem with SiB2: May–October 1987. *Journal of the Atmospheric Sciences*, **55**, 1141–1169.

Cowan IR, Farquhar GD (1977) Stomatal function in relation to leaf metabolism and environment. *Symposium of the Society for Experimental Biology*, **31**, 471–505.

Dang QL, Margolis HA, Collatz GJ (1998) Parameterization and testing of a coupled photosynthesis–stomatal conductance model for boreal trees. *Tree Physiology*, **18**, 141–153.

de Pury DGG, Farquhar GD (1997) Simple scaling of photosynthesis from leaves to canopies without the errors of big-leaf models. *Plant, Cell and Environment*, **20**, 537–557.

Dickinson RE (1983) Land surface processes and climate-surface albedos and energy balance. *Advances in Geophysics*, **25**, 305–353.

Doherty J (2002) *PEST: Model-Independent Parameter Estimation*, 4th Edn. Watermark Numerical Computing, Utah, USA.

Falge E, Tenhunen J, Baldocchi DD *et al*. (2001) Gap-filled strategies for defensible annual sums of net ecosystem exchange. *Agricultural and Forest Meteorology*, **107**, 43–69.

Federer CA (1982) Transpirational supply and demand: plant, soil, and atmospheric effects evaluated by simulation. *Water Resources Research*, **18**, 355–362.

Field C (1983) Allocating leaf nitrogen for the maximization of carbon gain: leaf age as a control on the allocation program. *Oecologia*, **56**, 341–347.

Field CB, Jackson RB, Mooney HA (1995) Stomatal responses to increasing CO_2: implications from the plant to global scale. *Plant, Cell and Environment*, **18**, 1214–1225.

Gill DS, Amthor JS, Bormann FH (1998) Leaf phenology, photosynthesis, and persistence of samplings and shrubs in a mature northern hardwood forest. *Tree Physiology*, **18**, 281–289.

Goulden ML, Munger JW, Fan SM *et al*. (1996) Exchange of carbon dioxide by a deciduous forest: response to interannual climate variability. *Science*, **271**, 1576–1578.

Granier A, Ceschia E, Damesin C *et al*. (2002a) The carbon balance of a young beech forest. *Functional Ecology*, **14**, 312–325.

Granier A, Pilegaard K, Jensen NO (2002b) Similar net ecosystem exchange of beech stands located in France and Denmark. *Agricultural and Forest Meteorology*, **114**, 75–82.

Hanan NP, Berry JA, Verma SB *et al*. (2005) Testing a model of CO_2, water and energy exchange in Great Plains tallgrass prairie and wheat ecosystems. *Agricultural and Forest Meteorology*, **131**, 162–179

Jackson RB, Canadell J, Ehleringer JR *et al*. (1996) A global analysis of root distributions for terrestrial biomes. *Oecologia*, **108**, 389–411.

Kaminski T, Knorr W, Rayner PJ *et al*. (2002) Assimilating atmospheric data into a terrestrial biosphere model: a case study of the seasonal cycle. *Global Biogeochemical Cycles*, **16**, 1066, doi: 10.1029/2001GB001463.

Kelly RH, Parton WJ, Hartman MD *et al*. (2000) Intra-annual and interannual variability of ecosystem process in shortgrass steppe. *Journal of Geophysical Research*, **105**, 20093–20100.

Kirschbaum MUF (1995) The temperature dependence of soil organic matter decomposition, and effect of global warming on soil organic matter storage. *Soil Biology and Biochemistry*, **27**, 753–760.

Kowalczyk EA, Garratt JR, Krummel PB (1994) *Implementation of a Soil-Canopy Scheme into the CSIRO GCM – Regional Aspects of the Model Response*. CSIRO, Melbourne (CSIRO Division of Atmospheric Research technical paper; no. 32).

Kramer K, Leinonen I, Loustau D (2000) The importance of phenology for evaluation of climate change on growth of boreal, temperate and Mediterranean forest ecosystems: an overview. *International Journal of Biometeorology*, **44**, 67–75.

Law BE, Fagle E, Gu L *et al*. (2002) Environmental controls over carbon dioxide and water vapor exchange of terrestrial vegetation. *Agricultural and Forest Meteorology*, **113**, 97–120.

Leuning R (1995) A critical appraisal of a coupled stomatal–photosynthesis model for C_3 plants. *Plant, Cell and Environment*, **18**, 339–357.

Leuning R (1997) Scaling to a common temperature improves the V_{cmax}. *Journal of Experimental Botany*, **307**, 345–347.

Leuning R (2002) Temperature dependence of two parameters in a photosynthesis model. *Plant, Cell and Environment*, **25**, 1205–1210.

Leuning R, Cleugh HA, Zegelin SJ *et al*. (2005) Carbon and Water Fluxes over a Temperate *Eucalyptus* Forest and a Tropical Wet/Dry Savanna in Australia: measurements and comparison with MODIS remote sensing estimates. *Agricultural and Forest Meteorology*, **129**, 151–173.

Leuning R, Kelliher FM, Depury DGG *et al*. (1995) Leaf nitrogen, photosynthesis, conductance and transpiration – scaling from leaves to canopies. *Plant, Cell and Environment*, **18**, 1183–1200.

Medlyn BE (1996) The optimal allocation of nitrogen within the C_3 photosynthetic system at elevated CO_2. *Australian Journal of Plant Physiology*, **23**, 593–603.

Meir P, Kruijt B, Broadmeadow M *et al*. (2002) Acclimation of photosynthetic capacity to irradiance in tree canopies in relation to leaf nitrogen concentration and leaf mass per unit area. *Plant, Cell and Environment*, **25**, 343–357.

Moncrieff JB, Malhi Y, Leuning R (1996) The propagation of errors in long-term measurements of land-atmosphere fluxes of carbon and water. *Global Change Biology*, **2**, 231–240.

Oechel WC, Ourlitis GL, Hastings SJ *et al*. (2000) Acclimation of ecosystem CO_2 exchange in the Alaska Artic in response to decadal climate warming. *Nature*, **406**, 978–981.

Pelkonen P, Hari P (1980) The dependence of springtime recovery of CO_2 uptake in Scots pine on temperature and internal factors. *Flora*, **169**, 398–404.

Pitman AJ (2003) The evolution of, and the revolution in, land surface schemes designed for climate models. *International Journal of Climatology*, **23**, 479–510.

Pitman AJ, Henderson-Sellers A, Desborough CE *et al*. (1999) Key results and implications from phase 1(c) of the Project for Intercomparison of Land-Surface Parameterization Schemes. *Climate Dynamics*, **15**, 673–684.

Raupach MR, Finkele K, Zhang L (1997) *SCAM (Soil–Canopy–Atmosphere Model): description and comparisons with field data*. CSIRO Centre for Environmental Mechanics Technical Report 32, Canberra, Australia.

Rayment MB, Loustau D, Jarvis PG (2002) Photosynthesis and respiration of black spruce at three organizational scales: shoot, branch and canopy. *Tree Physiology*, **22**, 219–229.

Reichstein M, Falge E, Baldocchi D *et al*. (2005) On the separation of net ecosystem exchange into assimilation and ecosystem respiration: review and improved algorithm. *Global Change Biology*, **11**, 1424–1439.

Seibt WA, Brand A, Heimann M *et al*. (2004) Observations of O_2: CO_2 exchange ratios during ecosystem gas exchange. *Global Biogeochemical Cycles*, **18**, GB4024, doi: 10.1029/2004GB002242.

Sellers PJ, Hall FG, Kelly RD *et al*. (1997) BOREAS in 1997: scientific results, overview and future directions. *Journal of Geophysical Research*, **102**, 28731–28769.

Sellers PJ, Randall DA, Collatz GJ *et al*. (1996) A revised land surface parameterization (SiB2) for atmospheric GCMs. Part II: generation of global fields of terrestrial biophysical parameters from satellite data. *Journal of Climate*, **9**, 706–737.

Spitters CJT (1986) Separating the diffuse and direct component of global radiation and its implications for modeling canopy photosynthesis. Part II: calculation of canopy photosynthesis. *Agricultural and Forest Meteorology*, **38**, 231–242.

Suni T, Rinne J, Reissell A *et al*. (2003) Long-term measurements of surface fluxes above a Scots pine forest in Hyytiala, southern Finland, 1996–2001. *Boreal Environment Research*, **8**, 287–301.

Tanaka K, Kosugi Y, Nakamura A (2002) Impact of leaf physiological characteristics on seasonal variation in CO_2, latent and sensible heat exchanges over a tree plantation. *Agricultural and Forest Meteorology*, **114**, 103–122.

Tjoelker MG, Oleksyn J, Reeich PB (2001) Modeling respiration of vegetation: evidence for a general temperature-dependent Q10. *Global Change Biology*, **7**, 223–230.

Valentini R, DeAngelis P, Matteucci G *et al*. (1996) Seasonal net carbon dioxide exchange of a beach forest with the atmosphere. *Global Change Biology*, **2**, 199–207.

Valentini R, Matteucci G, Dolman AJ *et al*. (2000) Respiration as the main determinant of carbon balance in European forests. *Nature*, **404**, 861–865.

Wang YP (2003) A comparison of three different canopy radiation models commonly used in plant modelling. *Functional Plant Biology*, **30**, 143–152.

Wang YP, Jarvis PG (1990) Influence of crown structural properties on PAR absorption, photosynthesis and transpiration in sitka spruce: application of a model (MAESTRO). *Tree Physiology*, **7**, 297–316.

Wang YP, Jarvis PG (1993) Influence of shoot structure on the photosynthesis of Sitka spruce (*picea sitchensis*). *Functional Ecology*, **7**, 433–451.

Wang YP, Leuning R (1998) A two-leaf model for canopy conductance, photosynthesis and partitioning of available energy I: model description and comparison with a multi-layered model. *Agricultural and Forest Meteorology*, **91**, 89–111.

Wang YP, Leuning R, Cleugh HA *et al*. (2001) Parameter estimation in surface exchange models using nonlinear inversion: how many parameters can we estimate and which measurements are most useful. *Global Change Biology*, **7**, 495–510.

Wang Q, Tenhunen J, Falge E *et al*. (2003) Simulation and scaling of temporal variation in gross primary production for coniferous and deciduous temperate forests. *Global Change Biology*, **10**, 37–51.

Willaims M, Scharz PA, Law BE *et al*. (2005) An improved analysis of forest carbon dynamics using data assimilation. *Global Change Biology*, **11**, 89–105.

Williams M, Rastetter EB, Fernandes DN *et al*. (1996) Modelling the soil-plant-atmosphere continuum in a Quercus-Acer stand at Harvard forest: the regulation of stomatal conductance by light, nitrogen and soil/plant hydraulic properties. *Plant, Cell and Environment*, **19**, 911–927.

Willmott CJ (1984) On the validation of models. *Physical Geography*, **2**, 184–194.

Wilson KB, Baldocchi DD (2000) Seasonal and interannual variability of energy fluxes over a broadleaved temperate deciduous forest in North America. *Agricultural and Forest Meteorology*, **100**, 1–18.

Wilson KB, Baldocchi DD, Aubinet M *et al*. (2002) Energy partitioning between latent and sensible heat flux during the warm season at FLUXNET sites. *Water Resources Research*, **38**, 1294, doi:10.1029/2001 WR000989.

Wilson KB, Baldocchi DD, Falge E *et al*. (2003) Diurnal centroid of ecosystem energy and carbon fluxes at FLUXNET sites. *Journal of Geophysical Research*, **108** (D21), 4664, doi: 10.1029/2001JD001349.

Wilson KB, Baldocchi DD, Hanson PJ (2001) Leaf age affects the seasonal pattern of photosynthetic capacity and net ecosystem exchange of carbon in a deciduous forest. *Plant, Cell and Environment*, **24**, 571–583.

Wofsy SC, Goulden ML, Munger JW *et al*. (1993) Net exchange of CO_2 in mid-latitude forests. *Science*, **260**, 1314–1317.

Wullschleger SD (1993) Biochemical limitations to carbon assimilation in C3 plants – a retrospective analysis of the A/Ci curves from 109 species. *Journal of Experimental Botany*, **44**, 907–920.

Xu LK, Baldocchi DD (2003) Seasonal trends in photosynthetic parameters and stomatal conductance of blue oak (*Quercus douglasii*) under prolonged summer drought and high temperature. *Tree Physiology*, **23**, 865–877.